

Crystallographic orientation analysis and high temperature strength of melt growth composite

S. Sakata*, A. Mitani, K. Shimizu, Y. Waku

UBE Industries, Ltd., 1978-5 Kogushi, Ube City, 755-8633 Yamaguchi, Japan

Available online 3 February 2005

Abstract

A unidirectional solidified $\text{Al}_2\text{O}_3/\text{YAG}$ binary melt growth composite (MGC) with 40 mm in diameter and 80 mm in length has been fabricated by the Bridgman method. In order to clarify crystallographic characteristics of the MGC fabricated, we carried out the crystal orientation analysis using pole figure measurement from two directions for two MGC ingots. The solidification directions of each ingot were almost $[1\ 1\ \bar{2}\ 0]$ Al_2O_3 and $[1\ 1\ 0]$ YAG, and $[0\ 1\ \bar{1}\ 0]$ Al_2O_3 and $[1\ 1\ 0]$ YAG, respectively. The same set of the crystal orientations which were $[0\ 0\ 0\ 1]$ Al_2O_3 and $[\bar{1}\ 1\ 2]$ YAG existed in the plane vertical to the solidification direction in two MGC ingots. Since the result of the crystal orientation analysis from two directions was corresponding, these MGC ingots were composed of a single Al_2O_3 crystal and a single YAG crystal. The relation of the crystal orientation between the Al_2O_3 phase and the YAG phase in one ingot agreed with previous studies on directionally solidified $\text{Al}_2\text{O}_3/\text{YAG}$ eutectic composites.

© 2005 Elsevier Ltd. All rights reserved.

Keywords: Unidirectional solidification; X-ray method

1. Introduction

A unidirectional solidified $\text{Al}_2\text{O}_3/\text{YAG}$ eutectic composite with 40 mm in diameter and 80 mm in length has been manufactured by the Bridgman method (BM) in UBE Industries, Ltd. We call this material as a Melt Growth Composite (MGC). Excellent mechanical properties of a MGC appear from the entanglement of a single Al_2O_3 crystal and a single YAG crystal, and no existence of amorphous phases at the interface between Al_2O_3 and YAG phases.¹ Since the existence of grain boundaries causes the decrease in the mechanical properties of an $\text{Al}_2\text{O}_3/\text{YAG}$ eutectic composite,² it is important that an ingot of a MGC is composed of a single Al_2O_3 crystal and a single YAG crystal without grain boundaries. The orientation analysis of Al_2O_3 and YAG phases in the MGC ingot is an effectual method for the confirmation of the quality of the MGC ingot. In the previous studies the orienta-

tion analyses of MGCs were done with TEM³ and X-ray⁴ but these were local analyses. In the $\text{Al}_2\text{O}_3/\text{YAG}$ eutectic composite made by the laser-heated float zone method (LHFZ), the crystal orientation analysis over the entire crystal rod has been done.⁵ This work gave some important information for understanding mechanical properties of the $\text{Al}_2\text{O}_3/\text{YAG}$ eutectic composite made by the LHFZ.⁶

In order to understand the excellent high temperature mechanical properties of the MGC made by the BM,^{7,8} crystallographic analysis over the entire MGC ingot are important. The Laue method is useful for studying the crystal orientation, but in case of MGC it needs to separate the diffraction pattern for each crystal. This method needs high skill to determine the crystal orientation in the MGC ingot. Therefore, the pole figure technique was applied to determine the crystal orientation of the MGC ingot. Because only the peak from a target crystal plane is observed in the pole figure measurement, it is most suitable method for the MGC ingot. We report on the analysis of the crystal orientation of the entire MGC ingot.

* Corresponding author.

E-mail address: 26676u@ube-ind.co.jp (S. Sakata).

2. Experimental

2.1. Unidirectional solidification

Commercially available Al_2O_3 powder (AKP-30, Sumitomo Chemical Co., Ltd., Tokyo, Japan) and Y_2O_3 powder (Y_2O_3 -RU, submicron-type, Shin-Etsu Chemical Co., Ltd., Tokyo, Japan) were mixed to give a mole ratio of $\text{Al}_2\text{O}_3/\text{Y}_2\text{O}_3 = 82/18$. Wet ball milling using ethanol was carried out to obtain a homogeneous mixed powder. The preliminary melting experiment of this powder at 1900°C for 10 min was performed in the Mo crucible heated by high-frequency induction heating under a pressure of 2.6×10^{-2} Pa of argon. The unidirectional solidification experiment was performed using the Bridgman-type equipment at the Japan Ultra-high Temperature Material Research Center. The ingot obtained by preliminary melting was inserted into the Mo crucible (40 mm in inside diameter by 200 mm in length) that placed in vacuum chamber, and a graphite susceptor was heated by high-frequency induction heating under a pressure of 2.6×10^{-2} Pa of argon. After holding for 30 min at 1900°C , unidirectional solidification was carry out by lowering the Mo crucible at speed of 5 mm h^{-1} in the same argon atmosphere. Since the seed crystal was not used in these solidification, the solidification direction of the MGC ingot was determined naturally.

2.2. Pole figure measurement

The obtained MGC ingot was cut in the plane vertical to the solidification direction and was made to semicylindrical shape in order to set on the stage of X-ray apparatus. The dimensions of the specimens were 40 mm in diameter by 10 mm in thickness. Two specimens were prepared from two different ingots of MGC. In this paper it called as ingot A and ingot B. The pole figure measurements were carried out with Rigaku RINT-2500 using Ni filtered $\text{Cu K}\alpha$ radiation. The divergence slit and receiving slit were 0.5° and 3 mm. Step size of pole angle (α) and azimuthal angle (β) are $2.0^\circ/\text{step}$. The measured crystal planes were (0 1 $\bar{1}$ 2), (1 0 $\bar{1}$ 4), (1 1 $\bar{2}$ 3), and (3 0 0 0) for the Al_2O_3 phase, (2 2 0), (4 0 0), and (4 2 2) for the YAG phase. Fig. 1 shows the radiation direction of X-ray and mounting orientation of a MGC ingot. The pole figure was

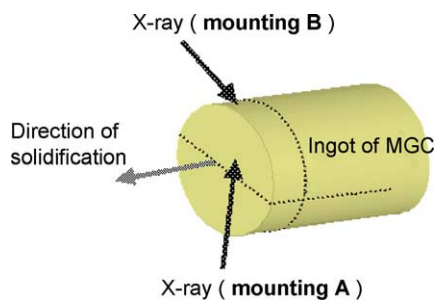


Fig. 1. Schematic drawing of the mounting of the specimen for pole figure measurement.

measured from two directions (mounting A and mounting B). The mounting A was for investigating the solidification direction and the mounting B was for investigating the crystal direction perpendicular to the solidification direction. From comparison of the results of the mounting A and mounting B, the crystal directions can be investigated in the whole ingot. “JSV1.08 lite” was used for drawing the stereographic projection.

3. Result and discussion

Fig. 2 shows an SEM image of the microstructure of a cross-section perpendicular to the solidification direction of an $\text{Al}_2\text{O}_3/\text{YAG}$ MGC ingot A. The light area in the SEM microstructure is the YAG phase, and the dark area is the Al_2O_3 phase. These phases entangle each other three-dimensionally. The dimensions of the YAG and Al_2O_3 phases are around $20\text{--}30 \mu\text{m}$ (this dimension is defined as the typical length of the short axis of each domain). Since the minimum irradiation area of X-ray is $1.0 \text{ mm} \times 0.8 \text{ mm}$ for pole figure measurement, it is enough area for the homogeneous measurement. Fig. 3 shows the examples of pole figure for specific crystal planes for the Al_2O_3 phase and the YAG phase in the MGC ingot A. The center of pole figure corresponds the solidification direction in the mounting A and the apex of specimens in the mounting B. These symmetric patterns indicate that the Al_2O_3 phase and the YAG phase are single crystals. The shape of each spot informs the crystal quality. Since the irradiated plane is not flat in the mounting B, it is essentially distorted. The spot of the (4 0 0) YAG plane in the mounting A (Fig. 3 (c)) is diffuse greatly, so the YAG phase in this ingot might contain subgrains. From these measurements the stereographic projection were drawn for each crystal for each mounting. The results are shown in Fig. 4. Each point was plotted from each measurement. For example, the point of the (1 0 0) and (0 1 0) YAG plane in Fig. 4 (d) were plotted

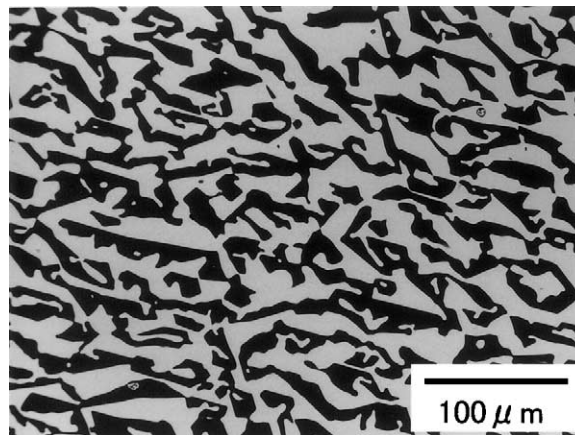


Fig. 2. SEM image showing the microstructure of a cross-section perpendicular to the solidification direction of the unidirectional solidified $\text{Al}_2\text{O}_3/\text{YAG}$ MGC ingot A.

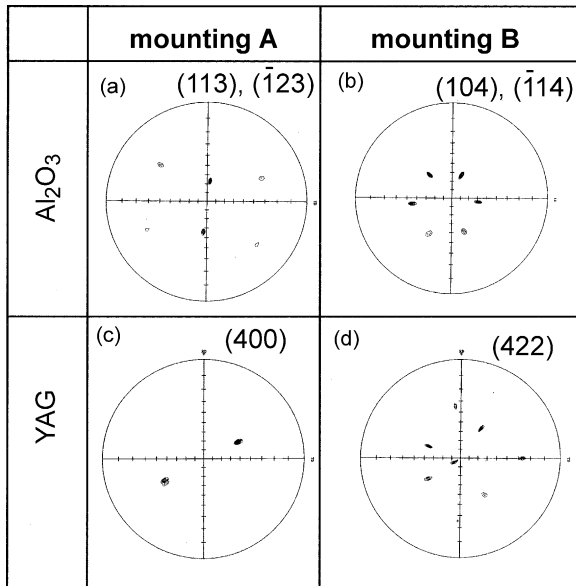


Fig. 3. Pole figures of the specific crystal plane for the Al₂O₃ and YAG phase for each mounting in the MGC ingot A.

from the pole figure of the (400) YAG plane in Fig. 3 (c). The solidification directions of the MGC ingot were determined from the result of the mounting A. Those were almost $[1\ 1\ \bar{2}\ 0]$ Al₂O₃ and $[1\ 1\ 0]$ YAG. The difference of the solidification direction and these directions was 3–4°. From the result of the mounting B the crystal directions perpendicular to the solidification direction were determined. The results are shown in Fig. 4 (b) and (e). The axis of $[0\ 0\ 0\ 1]$ Al₂O₃ and $[\bar{1}\ 1\ 2]$ YAG existed in the plane perpendicular to

the solidification direction and they were parallel. The stereographic projections of the mounting B forecast from the mounting A were corresponding to actual measurements that are indicated in Fig. 4 (b) and (e). As a preliminary explanation, the calculated stereographic projections are shown in Fig. 4 (c) and (f). These are projected from the solidification direction. For example, the angle between the (110) Al₂O₃ plane and the (001) Al₂O₃ plane is 90° and this relation corresponds to the result of the (110) Al₂O₃ plane in the mounting A and the (001) Al₂O₃ plane in the mounting B.

Fig. 5 shows the examples of pole figure for the MGC ingot B. These spot patterns also indicate that the Al₂O₃ phase and the YAG phase are single crystals respectively. Fig. 6 shows the stereographic projection of the Al₂O₃ phase for the MGC ingot B. Because the stereographic projection of the YAG phase was similar to that of the ingot A, it was omitted. The solidification direction of the MGC ingot B was almost $[0\ 1\ \bar{1}\ 0]$ Al₂O₃ and $[1\ 1\ 0]$ YAG. The difference angle between the solidification direction and these crystal directions was 7–11°. This difference is larger than that of the ingot A. There might be an offset angle. The crystal directions that were vertical to the solidification direction were $[0\ 0\ 0\ 1]$ Al₂O₃ and $[\bar{1}\ 1\ 2]$ YAG and they were parallel. The stereographic projections of the mounting B forecast from the mounting A were also corresponding to actual measurements that are indicated in Fig. 6 (b).

Fig. 7 shows summarized crystal orientations for the ingot A and the ingot B. It must be noted that these crystal orientations were determined from the measurement of

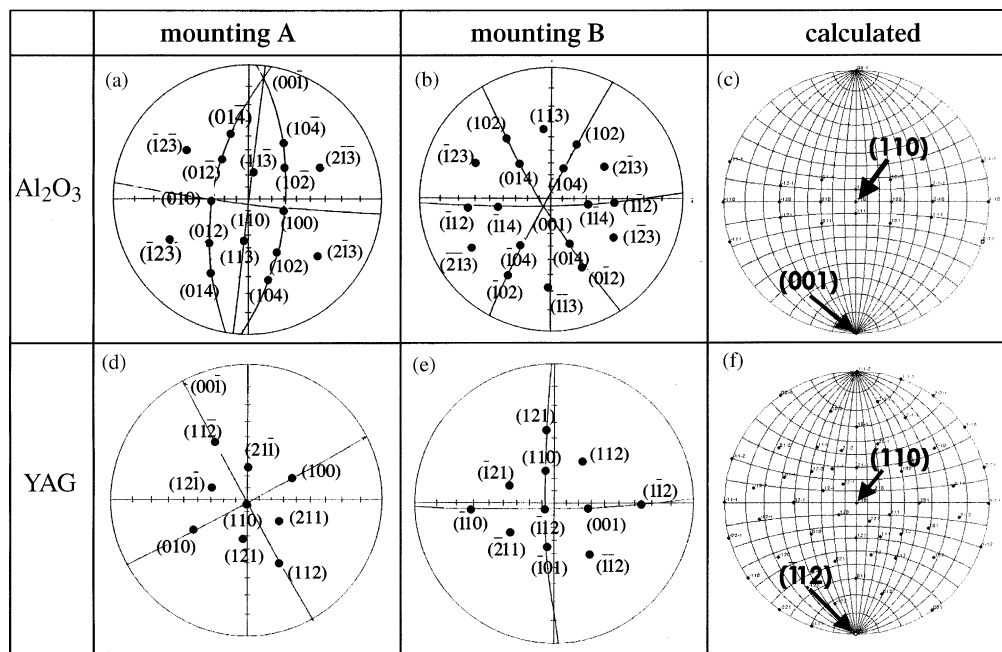


Fig. 4. (a, b, d and e) Stereographic projections for the Al₂O₃ and YAG phase for each mounting in the MGC ingot A. (c and f) Calculated stereographic projections for the Al₂O₃ and YAG crystals.

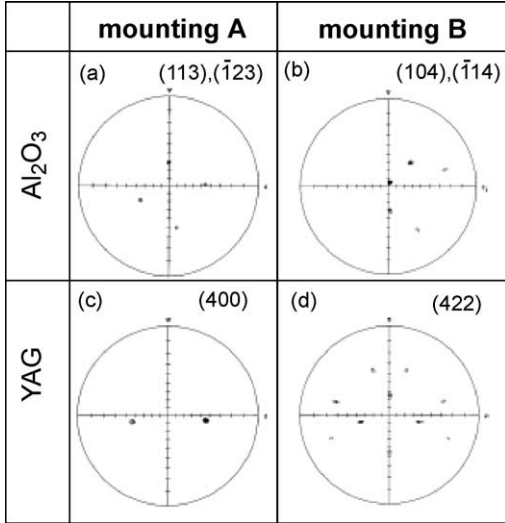


Fig. 5. Pole figures of the specific crystal plane for the Al₂O₃ and YAG phase for each mounting in the MGC ingot B.

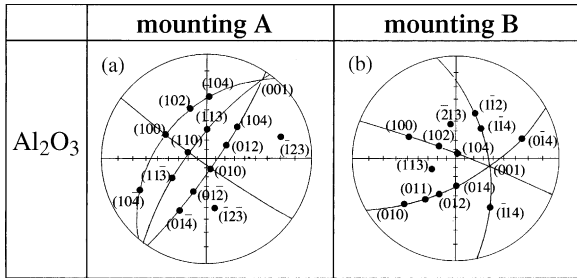


Fig. 6. Stereographic projections for the Al₂O₃ and YAG phase for each mounting in the MGC ingot B.

two different mountings. The measured MGC ingots were composed of a single Al₂O₃ crystal and a single YAG crystal throughout the ingot. The ingot A and the ingot B had the same directions that were [000 1] Al₂O₃ and [1̄ 1 2] YAG

and they were parallel. These directions were also found in our other MGC³ ingot. The combination of these crystal orientations was discussed from the viewpoint of the dislocation in the Al₂O₃ crystal.⁹ The relation of the crystal orientation between the Al₂O₃ phase and the YAG phase in the ingot A agreed with the previous studies.^{5,9} Based on the crystal orientation relationship of the ingot A, the crystal orientation of the Al₂O₃ phase in the ingot B rotated by 30° around the [1̄ 1 2] YAG axis. The symmetry of the Al₂O₃ single crystal might influence this angle.

The comparison with the texture and orientation analysis of the Al₂O₃/YAG eutectic composite made by the LHFZ⁵ will give important information about mechanical properties of MGCs. They have the different microstructure and mosaic structure. The average domain size in the MGC was larger than that made by the LHFZ. The difference of the domain size at center part and edge part in MGC ingot was small. This means the difference of the thermal gradient in the BM at a central part and the edge part is small. The mistilt of the growth direction between the Al₂O₃ phase and the YAG phase existed in the composite made by the LHFZ. This mistilt caused the mosaic structure in this composite. Since mistilt was small at the center part and large at the outer part, the mosaicity might change according to the radial position. On the other hand, there was no mistilt in the MGC ingot judging from the comparison of the crystal orientations for the mounting A and the mounting B. Additionally; the spot shape of the mounting A in Figs. 3 and 5 showed that the anisotropy of mosaicity was few. These results indicate that the mosaic structure in the MGC ingot is uniform. The uniformity of the microstructure and the mosaic structure are one reason that the MGC ingot has excellent mechanical properties at the high temperature. Such uniformities are caused from the uniformity of the temperature gradient in the BM.

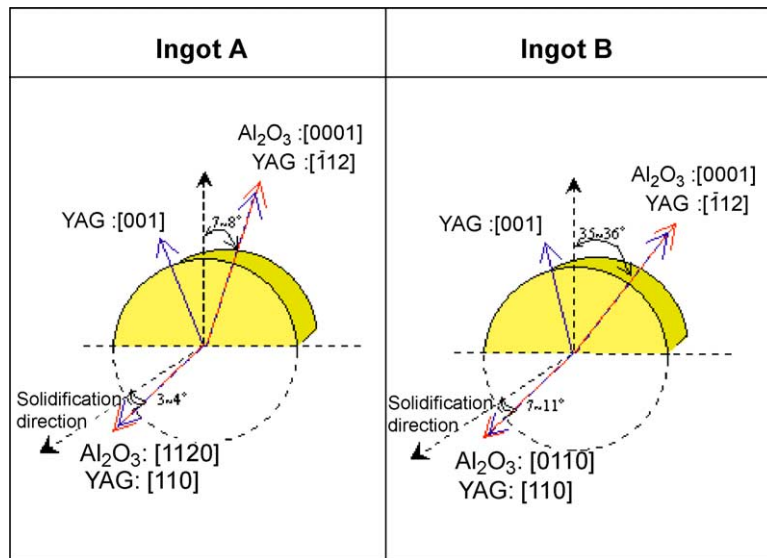


Fig. 7. Schematic drawing of the orientation of the MGC ingot A and ingot B.

4. Conclusions

The crystal orientation analysis of the MGC ingot with 40 mm in diameter manufactured by the Bridgman method was carried out with the whole ingot. Since the result of the crystal orientation analysis from two directions was corresponding, these MGC ingots were composed of a single Al_2O_3 crystal and a single YAG crystal. The solidification direction was different in each sample. The same set of the crystal orientations which were $[0001]$ Al_2O_3 and $[\bar{1}12]$ YAG existed in the plane vertical to the solidification direction for measured ingots. The microstructure and mosaic structure in the MCG ingot were homogeneous.

Acknowledgment

This study was performed through Special Coordination Funds of the Ministry of Education, Culture, Sports, Science and Technology of the Japanese Government.

References

1. Waku, Y., Unidirectional solidification of oxide eutectic ceramics. *Res. Adv. Appl. Phys. Global Res. Network*, 2001, **2**.
2. Parthasarathy, T. A., Mah, T.-I. and Matson, L. E., Deformation behavior of an $\text{Al}_2\text{O}_3\text{-Y}_3\text{Al}_5\text{O}_{12}$ eutectic composite in comparison with sapphire and YAG. *J. Am. Ceram. Soc.*, 1993, **76**, 29–32.
3. Yoshida, H., Shimura, K., Sugino, S., Ikuhara, Y., Sakuma, T., Nakagawa, N. et al., High-temperature deformation in unidirectionally solidified eutectic $\text{Al}_2\text{O}_3\text{-YAG}$ single crystal. *Key Eng. Mater.*, 2000, **171–174**, 855–862.
4. Waku, Y. and Sakuma, T., Dislocation mechanism of deformation and strength of $\text{Al}_2\text{O}_3\text{-YAG}$ single crystal composite at high temperature above 1500 °C. *J. Eur. Ceram. Soc.*, 2000, **20**, 1453–1458.
5. Frazer, C., Dickey, E. and Sayir, A., Crystallographic texture and orientation variants in $\text{Al}_2\text{O}_3/\text{Y}_3\text{Al}_5\text{O}_{12}$ directionally solidified eutectic crystals. *J. Cryst. Growth*, 2001, **233**, 187–195.
6. Sayir, A. and Matson, L. E., Growth and characterization of directionally solidified $\text{Al}_2\text{O}_3/\text{Y}_3\text{Al}_5\text{O}_{12}$ (YAG) eutectic fibers. In *Proceedings of the Fourth Annual HITEMP Review*. NASA Conference Publication, Cleveland, OH, 1991.
7. Waku, Y., Nakagawa, N., Wakamoto, T., Ohtsubo, H., Shimizu, K. and Kohtoku, Y., High-temperature strength and thermal stability of a unidirectionally solidified $\text{Al}_2\text{O}_3/\text{YAG}$ eutectic composite. *J. Mater. Sci.*, 1998, **33**, 1217–1225.
8. Waku, Y., Nakagawa, N., Wakamoto, T., Ohtsubo, H., Shimizu, K. and Kohtoku, Y., The creep and thermal stability characteristics of a unidirectionally solidified $\text{Al}_2\text{O}_3/\text{YAG}$ eutectic composite. *J. Mater. Sci.*, 1998, **33**, 4943–4951.
9. Hay, R. S. and Matson, L. E., Alumina/yttrium–aluminum garnet crystallographic orientation relationships and interphase boundaries: observations and interpretation by geometric criteria. *Acta Metall. Mater.*, 1991, **39**, 1981–1994.